Article ID: 1004-924X(2001)05-0411-07

# EUV Optical Design
## – Reflective and Diffractive Optics

Takeshi Namioka

*(Tohoku University, Japan)*

**Abstract:** This article describes the task of optical designers to achieve a better design. This is followed by some discussions on the necessity of total design that takes all the elements into account from its light source to the final image plane. Methods are given to simulate rays from a bending magnet and an undulator, surface figure errors, and thermal deformations. Some examples are given for an undulator beamline and an EUVL optical system, together with tolerance estimates of the figure error and thermal deformation.

**Key words:** optical design; ray-tracing; optical systems
**CLC number:** TH703 **Document code:** A

## 1 Introduction

A client often asks his designer for too much: excessive functions in one for cost saving, unrealistic high accuracy and performance just for self-satisfaction, for example. At the same time, it is also true that some clients provide exciting and challenging opportunities to designers and engineers.

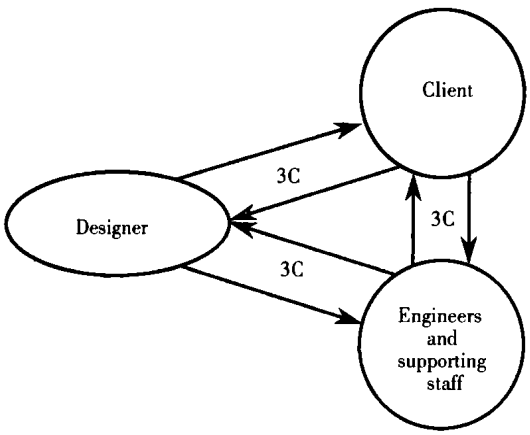


Fig. 1 Task of optical designers in achieving a better design

Designers also fall into a trap sometimes: the design itself is excellent but it cannot be materialized. This is because they have paid no attention to the present state of our technologies. In order to achieve a better design, it is important to have good relationship among the client, designer, and a group of engineers. Such a relation can be established only through "3C", i.e., "Communication, Collaboration, and Cooperation." This is illustrated in Fig. 1.

Here, communication means information exchange and discussion. Collaboration is to work together in scientific and/or technical subject. Cooperation signifies working together for a common purpose. These 3C facilitate a better understanding of the problems in the design work and realization of the best possible design under the state of the art. Thus, the 3C would lead to realistic specifications, a better design, and production of a desired system with everyone's satisfaction. In other words, the establishment of good 3C is the designers' most important task.

We now turn our subject to design work. Several good design codes like CODE V are now commercially available. Therefore, anyone can design visible/ultraviolet optics, to a certain extent, without too much trouble.

**Received date:** 2001-08-29; **revised date:** 2001-10-08

By contrast, soft-X-ray (SXR) optics must satisfy very stringent metrological requirements not usual to conventional optical elements used at longer wavelengths. This is due to short operating wavelengths. Thus, the effects of slope error, thermal deformation, etc. of each component cannot be ignored in the design of SXR optics. Furthermore, special attention should be directed to the rms source size and angular distributions of synchrotron radiation (SR) and undulator radiation (UR) because these new light sources are playing an important role in modern SXR researches.

In view of these facts, we can see clearly that in the design of an SXR optical system, the characteristics of all the elements of the system, from its light source to the final image plane, must be taken into account. This is the concept of "Total Design." We also see that it is important to have a convenient method for estimating tolerances for slope error and thermal deformation, besides the method commonly used to estimate tolerances for focal depth, assembling errors as decenter, tilt, despace, etc.

In the following we discuss the characteristics of SR/UR and the formulation of figure errors, slope errors, and thermal deformation of an ellipsoidal mirror. Then, we estimate tolerances for these errors. Examples are given in the cases of EUVL optics and undulator beamline optics.

## 2 Generation of rays in tracing

In performing ray tracing, rays should be generated randomly in accordance with the angular distribution of a given light source. For this, it is convenient to assume that the source comprises a number of point sources.

For a planar source radiating uniformly from every point in the source to all directions, we generate a uniformly random number sequence, $u_1$, $u_2$, $u_3$, …, in an interval [0, 1] and select source points in accordance with

$$s_i = W(u_i - 0.5) \text{ and } z_i = H(u_{i+1} - 0.5) \tag{1}$$

Here, the coordinate $(0, s_i, z_i)$ of a point $A_i$ is defined in the source plane, and $W$ and $H$ are the total width and height of the rectangular planar source, respectively. For a circular source, we use polar coordinates. In a similar manner, radiating angles are also determined randomly.

However, planar sources are not uniform in most cases and have certain distributions. SR and UR sources are good examples of this. We, therefore, have to take such distribution into account in the design of an optical system on an SR/UR beamline.

We consider a planar source having *double-Gaussian distributions* both in the position of and the radiating angles from point sources. A double-Gaussian distribution is expressed as

$$f(x, y) = \frac{1}{2\pi\sigma_1\sigma_2\sqrt{1-\rho^2}} \cdot \exp\left[\frac{1}{2(1-\rho^2)}\left(\frac{x^2}{\sigma_1^2} - \frac{2\rho xy}{\sigma_1\sigma_2} + \frac{y^2}{\sigma_2^2}\right)\right] \tag{2}$$

where, $\sigma_1^2$ and $\sigma_2^2$ are the variances of $x$ and $y$, and $\rho$ is the coefficient of correlation between $x$ and $y$. In the case of SR/UR, $\sigma_1$ and $\sigma_2$ are the rms transverse size of the electron beam in the horizontal and vertical directions, respectively, and $\rho$ can be set to zero.

Normal random numbers of two variables $(x_i, y_i)$ that have a probability density given by Eq. (2) are obtained by

$$x_i = \sigma_1\sqrt{-2\log_e u_i}\{\sqrt{1-\rho^2}\cos(2\pi u_{i+1}) + \rho\sin(2\pi u_{i+1})\},$$
$$y_i = \sigma_2\sqrt{-2\log_e u_i}\sin(2\pi u_{i+1}) \tag{3}$$

where, $u_i$ and $u_{i+1}$ are adjacent members of a uniformly random number sequence $\{u_i\}$ generated in an interval [0, 1]. The positions of point sources $A_i(0, s_i, z_i)$ are determined randomly from

$$s_i = W(x_i - 0.5) \text{ and } z_i = H(y_i - 0.5). \tag{4}$$

When the radiating angles of rays have a double-Gaussian distribution similar to Eq. (2) with $\sigma'_1$, $\sigma'_2$ and $\rho'$, the 3-D polar coordinates $(1, \varphi, \theta)$ of a radiating ray are determined from

$$\varphi = 2\pi x'_i \text{ and } \theta = \pi(y'_i - 0.5) \quad (5)$$

where $(x'_i, y'_i)$ are the normal random numbers obtained from

$$x'_i = \sigma'_1 \sqrt{-2\log_e u_{i+2}}$$
$$\{\sqrt{1-\rho'^2}\cos(2\pi u_{i+3}) + \rho\sin(2\pi u_{i+3})\},$$
$$y'_i = \sigma'_2 \sqrt{-2\log_e u_{i+2}}\sin(2\pi u_{i+3}) \quad (6)$$

In the case of SR/UR, $\sigma'_1$ and $\sigma'_2$ are the rms angular divergence of the electron beam in the horizontal and vertical directions, respectively, and $\rho'$ can be set to zero.

## 3 Surface figure of an ellipsoidal mirror

We consider the surface figure $\xi$ of an ellipsoidal mirror with the rms figure error $\Delta\xi_{FE}$ and rms thermal deformation $\Delta\xi_{TD}$:

$$\xi = a - a\sqrt{1-\left(\frac{w^2}{b^2} + \frac{l^2}{c^2}\right)} + \Delta\xi_{FE} + \Delta\xi_{TD} \quad (7)$$

### A. Figure error

The figure error is often represented by the values of slope error. We assume that the slope errors $s_y$ and $s_z$ at a point $P(\xi, w, l)$ on the mirror are distributed randomly with a probability density function

$$f(s_y, s_z) = \frac{1}{2\pi\sigma_1\sigma_2}\exp\left[-\frac{1}{2}\left(\frac{x^2}{\sigma_1^2} + \frac{y^2}{\sigma_2^2}\right)\right] \quad (8)$$

where $\sigma_1$ and $\sigma_2$ are the standard deviations of $s_y$ and $s_z$, respectively. We assume here that (1) $s_y$ and $s_z$ have no mutual correlation and (2) their respective averages over the mirror surface are zero.

The sequence $\{(s_y, s_z)_i\}$ of normal random slope errors with the probability density of Eq. (8) are generated from

$$(s_y)_i \equiv \left[\frac{\partial(\Delta\xi_{FE})}{\partial w}\right]_i =$$
$$\sigma_1\sqrt{-2\log_e u_i}\cos(2\pi u_{i+1}),$$
$$(s_z)_i \equiv \left[\frac{\partial(\Delta\xi_{FE})}{\partial l}\right]_i =$$
$$\sigma_2\sqrt{-2\log_e u_i}\sin(2\pi u_{i+1}) \quad (9)$$

with the aid of the sequence $\{u_i\}$ of uniform random numbers on the interval [0, 1].

The corresponding figure error $\Delta\xi_{FE}$ is then obtained by integrating

$$d(\Delta\xi_{FE})_i \equiv (s_y)_i dw + (s_z)_i dl \quad (10)$$

under an assumption $\sigma_1 = \sigma_2 \equiv \sigma_{SE}$:

$$(\Delta\xi_{FE})_i = \sigma_{SE}\sqrt{-2\log_e u_i}$$
$$[w\cos(2\pi u_{i+1}) + l\sin(2\pi u_{i+1})]. \quad (11)$$

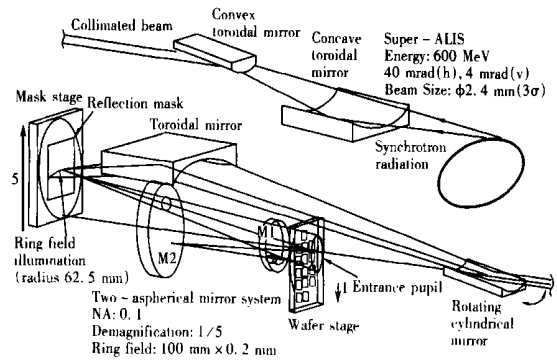


Fig. 2 Schematic diagram of an EUVL optical system

We show an example of figure-error calculations as applied to a double-mirror system for EUVL, which is illustrated in Fig. 2. In the calculations we consider a 2-D array of 0. 5μm line-and-space pattern on the mask (see Fig. 3) and assume that the space portions of this grid pattern emit light into the entrance pupil of the system. Rays originating from each one of the nine spaces are traced through the convex ellipsoidal mirror M1 and the concave ellipsoidal mirror M2, assuming various values of rms slope errors for M1 and M2. Figure 4 shows images of the mask pattern constructed by ray tracing for $\sigma_{SE}(M1) = 0.05, 0.1, 0.2$μrad with $\sigma_{SE}(M2) = 0$. The values $\sigma_{SE}(M1) = 0.05$, 0. 1 and 0. 2μrad correspond to the rms figure errors $\Delta\xi_{FE}(M1) = 0.56$nm, 1. 13nm, and 2. 24nm, respectively. Figure 4 clearly shows the effect of slope errors on the pattern resolution. More details will be discussed in Section 4.

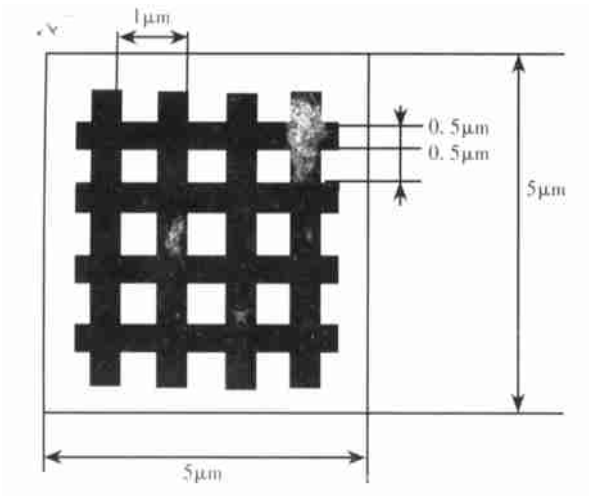


Fig. 3　Source pattern on the mask

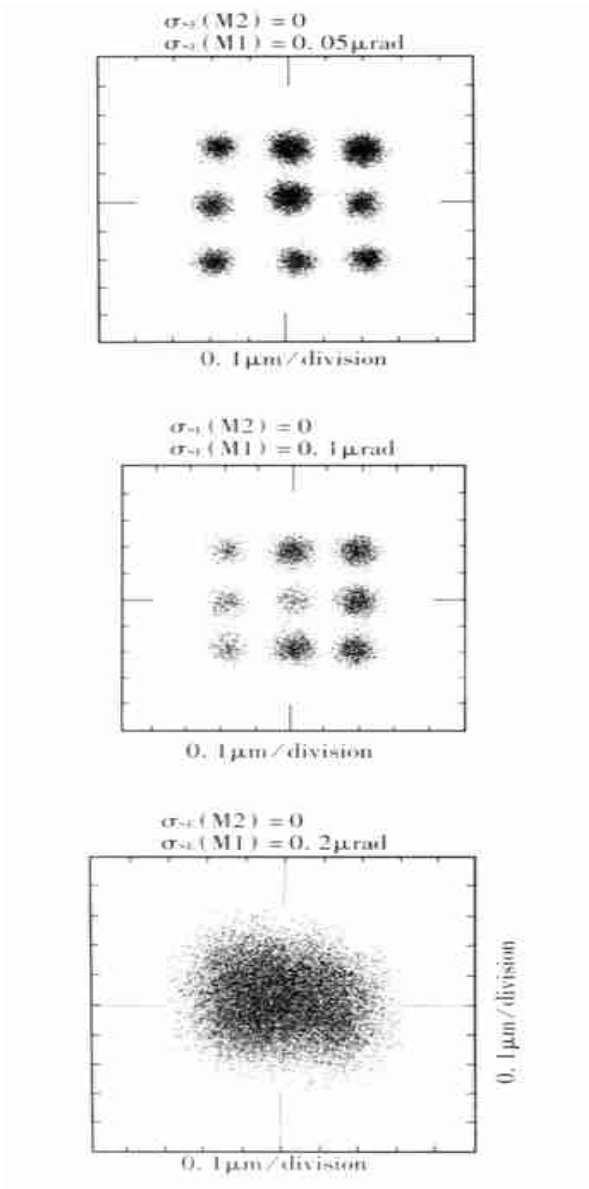


Fig. 4　Mask-pattern images constructed by ray tracing

**B. Thermal deformation**

The heat load exerted on beamline optics by UR can distort their surfaces. The effect is the greatest on the first element, usually a mirror.

We can calculate such a thermally deformed mirror surface in four steps:

(1) calculation of power density output of the assumed undulator for individual harmonics by URGENT, a code for calculating UR properties,

(2) calculation of absorbed harmonic power densities on the mirror surface by URGENT,

(3) calculation of thermal deformation of the mirror substrate by means of a finite-element method (ANSYS, a commercial code), and

(4) curve fitting of the deformed surface figure to a polynomial of the form

$$\Delta\xi_{TD}(w,l)=\sum_{i,j}A_{ij}w^{i}l^{j},\ 0\leqslant i+j\leqslant 6 \tag{12}$$

where $A'_{ij}$ s are the deformation coefficients.

Using URGENT and ANSYS we simulated the thermal surface-deformation of a water-cooled Ni-coated spherical Glidcop$^{TM}$ mirror exposed to UR at an angle of incidence of 87°. URGENT calculation shows that the mirror receives a total power of 209W and absorbs 127W on its surface. The result of ANSYS calculation are curve fitted to Eq. (7) upon substitution of Eq. (12) and $\Delta\xi_{FE}=0$. This yields the thermally deformed surface of the spherical mirror as

$$\begin{aligned}\xi=\ & R-R\sqrt{1-(w^2+l^2)/R^2}+3.09499\times10^{-4}-\\ & 3.39872\times10^{-8}w^2-8.21102\times10^{-8}l^2+\\ & 4.75112\times10^{-12}w^4+4.833510\times10^{-11}w^2l^2-\\ & 4.880480\times10^{-7}l^4-3.812470\times10^{-16}w^6-\\ & 1.569350\times10^{-14}w^4l^2+5.484390\times10^{-12}w^2l^4+\\ & 2.030340\times10^{-8}l^6,\end{aligned} \tag{13}$$

where $R=a=b=c$ is the radius of curvature of the mirror. Figure. 5 shows the deformation of the mirror surface due to UR power loading. With the aid of Eq. (13) we can carry out ray tracing through an optical system on an undulator beamline whose first mirror is thermally deformed and evaluate the performance of the beamline optics.

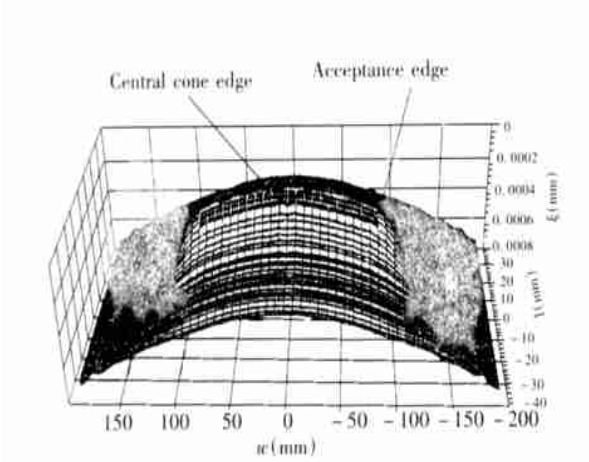


Fig. 5 Deformation of the mirror surface due to undulator power loading

## 4 Tolerance estimation

It is important in any design work to estimate the tolerance of various quantities. In this section we describe, as an example, the tolerance estimates for figure errors of an EUVL double-mirror system and those for slope errors and thermal deformations of the first mirror of an SXR monochromator on an undulator beamline.

**A. EUVL double-mirror system**

We consider the optics of Fig. 2 and the mask pattern of Fig. 3 and estimate the tolerance for figure-errors/slope-errors of the ellipsoidal mirrors M1 and M2. Square-wave MTF (Modulation Transfer Function) calculations made for this system with ideal M1 and M2 indicate that the system would provide 0.1μm spatial resolution if the modulation in the pattern profiles exceeds 45% at a spatial frequency of 5000 cycles/mm. We therefore adopt 45% modulation in the profiles of spot diagrams as a criterion for 0.1μm resolution.

To estimate the tolerance for the figure error, we construct spot diagrams by tracing rays through the system with various values of slope errors for M1 and M2. Then, the intensity profiles of imaged pattern are constructed from the spot diagrams, and the degree of their modulations is examined.

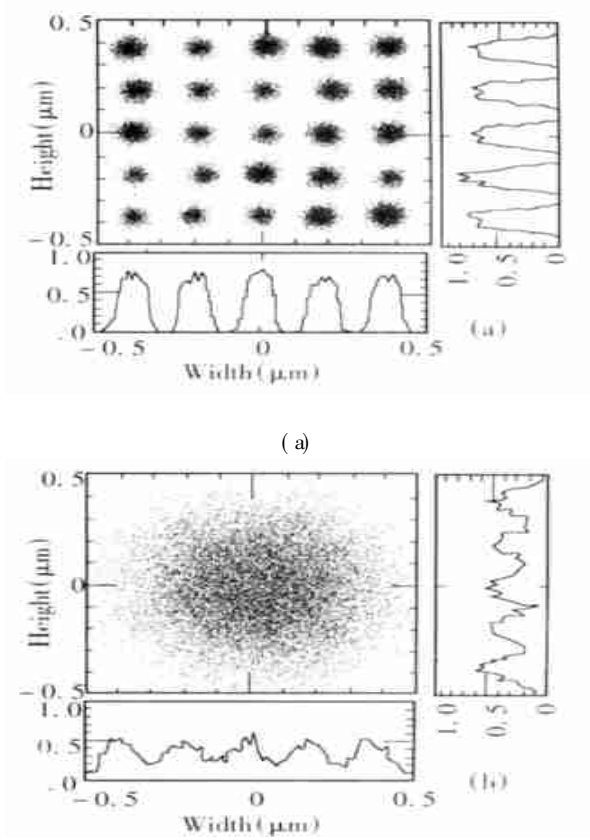


Fig. 6 Spot diagrams and their pattern profiles (a) $\sigma_{SE}$ (M1, M2) = 0, (b) $\sigma_{SE}$ (M1, M2) = 0.05μrad

Fig. 6 shows the spot diagrams and their pattern profiles thus obtained in the cases of (a) $\sigma_{SE}$ (M1, M2) = 0μrad (i.e., ideal case) and (b) $\sigma_{SE}$ (M1, M2) = 0.05μrad. The modulation of the pattern profiles in case (b) is estimated to be ~ 40%, a value slightly less than the criterion. It was also found that the pattern profiles constructed for $\sigma_{SE}$ (M1) = 0.1μrad and $\sigma_{SE}$ (M2) = 0.05μrad were almost indistinguishable from those of case (b). This and other similar results indicate that the pattern profiles are governed by the rms slope error of M2, but not much by that of M1. Considering these findings together with the result that the modulation well exceeds 50% for $\sigma_{SE}$ (M1, M2) = 0.04μrad, we adopt $\sigma_{SE}$ (M1) = 0.1μrad and $\sigma_{SE}$ (M2) = 0.04μrad as the tolerance. With the aid of Eq. (11), the rms surface figure errors are estimat-

ed to be $\Delta\xi_{FE}$ (M1) = 1.2nm and $\Delta\xi_{FE}$ (M2) = ~ 1.5nm.

The surfaces of the fabricated M1 and M2 were measured with an interferometer, and their rms figure errors were found to be ~ 1.8 nm for M1 and ~ 1.5 nm for M2. From these values the rms slope errors were derived as $\sigma_{SE}$ (M1) = 0.1μrad and $\sigma_{SE}$ (M2) = 0.06μrad. Our simulation values, if valid, indicate a fair chance of getting a spatial resolution close to 0.1μm with this EUVL optics. Experiment performed with this system showed a resolution much better than 0.5μm all over an area of 10mm × 10mm on the wafer, supporting the adequacy of our tolerance estimation.

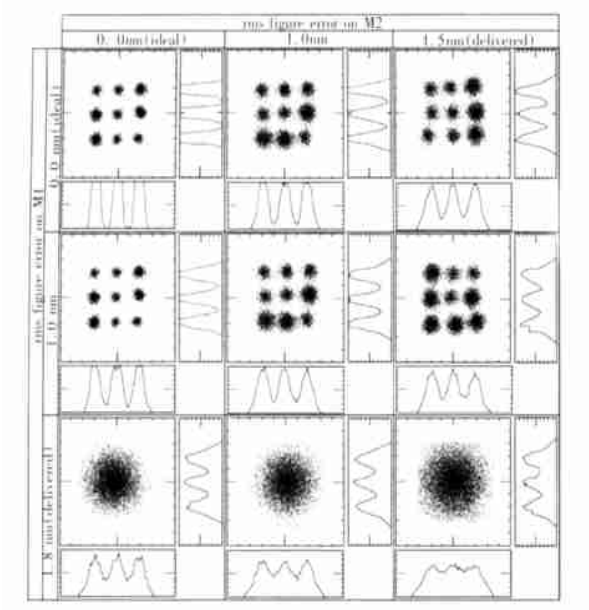


Fig. 7 Effect of the rms figure errors of M1 and M2 on the spatial resolution of the system

For the readers' interest, Fig. 7 is attached to show the effect of the rms figure errors of M1 and M2 on the spatial resolution of the system. In the figure, spot diagrams and pattern profiles are given for $\Delta\xi_{FE}$ (M1) = 0, 1.0, 1.8nm and $\Delta\xi_{FE}$ (M2) = 0, 1.0, 1.5nm.

**B. Undulator beamline optics**

We evaluate the effects of slope errors and thermal deformations by taking a Monk-Gillieson monochromator on an undulator beamline (see Fig. 8). A concave mirror M accepts radiation from an undulator U and produces a converging beam onto a plane grating G. The thermally deformed mirror M is assumed to have the surface figure expressed by Eq. (13). In performing ray tracing through the monochromator, the same machine parameters as those used to derive Eq. (13) are employed.

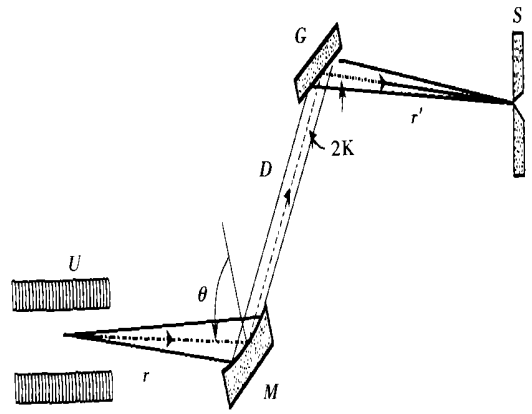


Fig. 8 Schematic diagram of a Monk-Gillieson monochromator on an undulator beamline. U, undulator; M, water-cooled metal concave mirror of 75m radius of curvature; G, varied line spacing plane grating having a groove density of 2400 lines/mm; S, exit slit; $r$ = 17 m; θ = 87°; D = 200mm; $r'$ = 2032mm; $2K$ = 170°.

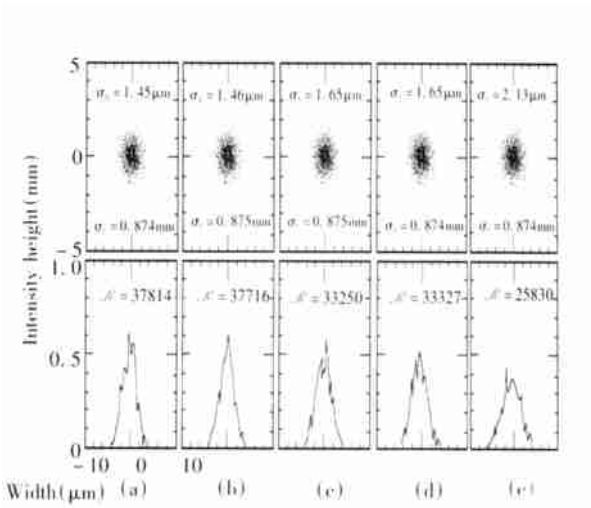


Fig. 9 Spot diagrams and line profiles. The mirror is assumed to have (a) a deformed surface of Eq. (13), (c) a deformed surface of Eq. (13) with $\sigma_{SE}$ = 1μrad, (d) $\Delta\xi_{FD}$ = 0 and $\sigma_{SE}$ = 1μrad, or (e) $\Delta\xi_{FD}$ = 0 and $\sigma_{SE}$ = 2μrad.

Figure 9 illustrates the result of ray tracing made under the assumption that M has (a) ideal surface, (b) a deformed surface of Eq. (13), (c) a deformed surface of Eq. (13) with $\sigma_{SE}$ = 1μrad, (d) $\Delta\xi_{FD}$ = 0 and $\sigma_{SE}$ = 1μrad, or (e) $\Delta\xi_{FD}$ = 0 and $\sigma_{SE}$ = 2μrad.

It is evident from Fig. 9 that M would not cause significant degradation in spectral images regardless of thermal deformation, so long as its slope error is kept smaller than~ 1μrad. This suggests that the performance of the monochromator is nearly source size limited. Thus, the water-cooled metal mirror M would withstand heat load exerted by the undulator without affecting the image quality.

For the undulator considered here, we may take, therefore, 1μrad as the tolerance for the rms slope error of M. When the undulator is operated with different machine parameters so as to give a source size several times smaller than considered above, the resolving power and throughput of the monochromator no longer become source size limited. This results in tighter tolerance both for thermal deformation and for slope error.